Basket-shaped quinacridone cyclophanes: synthesis, solid-state structures, and properties†

Dingyi Yu, Tai Peng, Hongyu Zhang,* Hai Bi, Jingying Zhang and Yue Wang*

Received (in Montpellier, France) 15th January 2010, Accepted 29th April 2010
DOI: 10.1039/c0nj00028k

A series of basket-shaped quinacridone (QA) cyclophanes **1–6** has been synthesized and characterized. Single-crystal X-ray analysis of **5** shows no infinite π–π aggregation between QA cores, reflecting a significant isolated effect of the bridging tethers. Photophysical properties have been carefully investigated. All cyclophanes show much higher quantum yields in concentrated solutions compared to the non-bridged QA analogue **7**. Further application of **1** as a green dopant in EL devices exhibits current efficiencies of 11.2 and 7.2 cd A^{-1} with doping concentrations of 0.5 and 3 wt%, respectively. QA cyclophanes maintain a high luminescent yield in both concentrated solution and high doping concentration EL devices, verifying that the basket-shaped functionalization is an ideal strategy for depressing fluorescence quenching of QA dyes in the condensed phase.

Introduction

Quinacridone (QA) and its derivatives have attracted considerable attention in recent years for their potential application in organic photovoltaics (OPVs) and organic light-emitting diodes (OLEDs) due to their excellent thermal, chemical, and photochemical stability.[1] However, these molecules possessing extended π-conjugation and rigid planarity readily aggregate with neighboring molecules in condensed phases, hence, dramatically decreasing not only their solubility but also the luminescent efficiencies in concentrated solutions or solid states. For instance, the unsubstituted QA compound is not soluble in common organic solvents and nonemissive in the solid state. Thus, QA dyes are often used as a fluorescent guest in OLEDs with very low doping concentrations.[2–8] Recently, some studies on QA dyes have been focused on the modification of this class of pigments with an aim to develop novel functional materials. Müllen and co-workers have carefully studied the phase-formation behavior and aggregation properties of some soluble QA derivatives.[2] Nakahara and co-workers have synthesized QA derivatives with four alkyl chains and used them in Langmuir–Blodgett films to control the orientation and packing of the chromophores.[1c,d] We have also carried out studies aimed at understanding how supramolecular organization in the solid state and solution affects the photoluminescent and electroluminescent properties of QA derivatives.[9,10]

The photophysical properties of a given fluorophore in the condensed phases, such as absorption and fluorescence emission, undergo significant variation according to the mode of molecular packing.[11–13] It has been revealed that strong intermolecular π–π interaction or continuous intermolecular hydrogen bonding between neighboring fluorophores is a principal factor of fluorescence quenching in concentrated solutions or solid states. In this regard, a promising approach to design intensively fluorescent dyes is to weaken/remove the intermolecular interactions between fluorophores in the condensed phases. In particular, the introduction of bulky substituents to the original fluorophores is known to be a very useful method for solving the problem of fluorescence quenching by aggregation.

A number of QA derivatives containing long alkyl chains at the *N*,*N*′ positions have been synthesized and characterized. This type of functionization indeed greatly improved the solubility and depressed the fluorescent quenching of QA dyes (Scheme 1). However, the flat conformations of QA derivatives enable these molecules have enough free space to π-stack with each other and hence form infinite aggregation. Therefore, to achieve highly emissive QA dyes in condensed

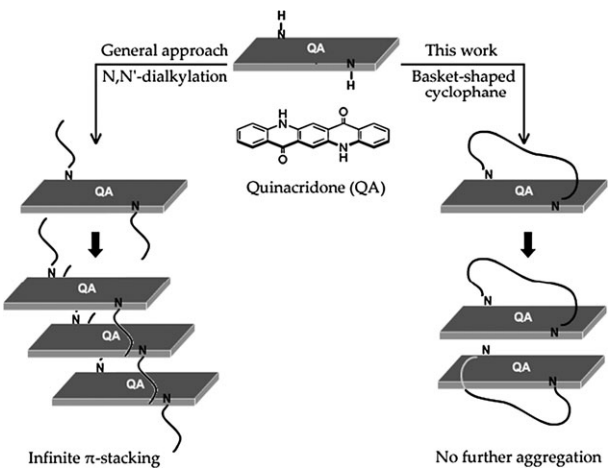

Scheme 1 Functionalization of quinacridone.

State Key Laboratory of Supramolecular Structure and Materials, College of Chemistry Jilin University, Changchun 130012, P. R. China. E-mail: yuewang@jlu.edu.cn, hongyuzhang@jlu.edu.cn; Fax: +86-431-85193421; Tel: +86-431-85168484

† Electronic supplementary information (ESI) available: Photophysical data, details of X-ray structures, and ^{1}H NMR spectra. CCDC reference number 759654. For ESI and crystallographic data in CIF or other electronic format see DOI: 10.1039/c0nj00028k

phase, the development of a novel design approach that can more effectively inhibit the intrinsic π-aggregation of QA cores is significantly important. Herein, we reported a novel design strategy to functionalize the QA core by connecting both N atoms with a long alkyl tether (Scheme 1). It is expected that the basket-shaped structure can efficiently keep the fluorophore π-system apart, thus dramatically enhance their luminescent efficiency in the condensed phases. To test this hypothesis, X-ray crystal structures, detailed photophysical properties, concentration-dependent fluorescence quantum yield and electroluminescent properties have been fully investigated.

Results and discussion

Synthesis and characterization

The basket-shaped QA cyclophanes **1–6** were synthesized by a simple one-step reaction of quinacridone (QA), 1,3,8,10-tetramethylquinacridone (TMQA), or 2,9-ditertubitylquinacridone (DBQA) with 1.0 mol amount of corresponding dibromides in the presence of sodium hydride in THF, as outlined in Scheme 2. Notably, the concentrations of the parent compounds are crucial regarding the yields of the target compounds. At higher concentration, the major products are *N*,*N*′-disubstituted QA derivatives which were formed by a double N-alkylation, and only trace amount of basket-shaped cyclophanes were isolated. We have found that the best way to maximize the production of basket-shaped QA cyclophanes is to add a dilute solution of dibromide to a dilute solution of QA precursors. When the reaction is performed in this way, one can obtain the cyclophanes in better isolated yields (15–22%). All these compounds were isolated by column chromatography and their structures were characterized by ^{1}H NMR, mass spectra, elemental analysis, and/or X-ray crystallography. In addition, the length of the alkyl chain of dibromides is important in terms of the formation of QA cyclophane. For instance, a reaction of QA with 1,8-dibromooctane in the same condition as mentioned above can not produce the target cyclophane.

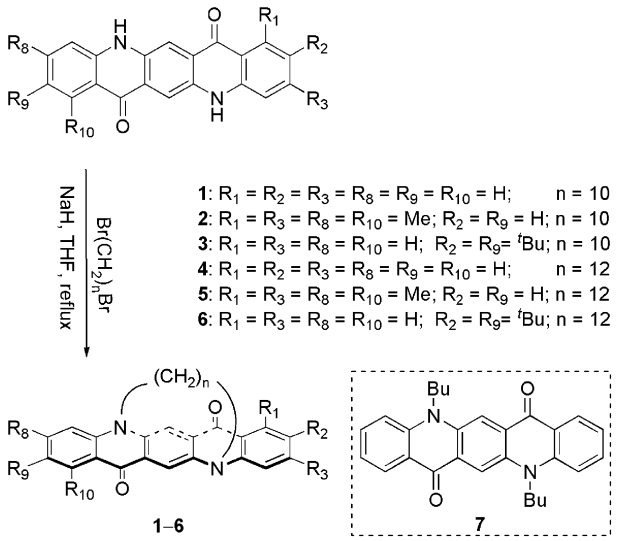

Scheme 2 Synthetic route for QA cyclophanes **1–6**.

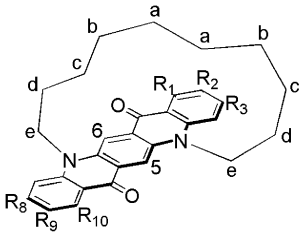
QA cyclophanes **1–3**

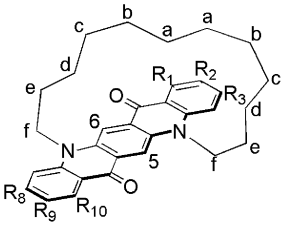
QA cyclophanes **4–6**

^{1}H NMR spectra of the QA cyclophanes **1–6** demonstrate that their molecular geometries are all centrosymmetric in solution. The ^{1}H NMR spectra and the fragmentation patterns on GC-MS mass spectra manifested their basket-shaped structure. Selected ^{1}H NMR chemical shifts of QA cyclophanes **1–6** and non-bridged reference **7** are summarized in Table 1. The well known shielding effect of aromatic rings on suitable located protons causes the peaks of the central methylene protons to appear at unusually high field.[14] The chemical shifts of the central methylene protons are in the range of 0.13–0.28 ppm for cyclophanes **1–3** and 0.26–0.37 for cyclophanes **4–6**, respectively, which are greatly high-field shifted compared to the highest chemical shift of the methylene proton of **7** (1.12 ppm). This comparison demonstrates the QA nucleus exerts a strong magnetic anisotropic effect on the chemical shifts of bridging tethers.

Solid-state structures

The structures of these QA cyclophanes were further confirmed by X-ray crystal analysis. Suitable crystals of 12C tether bridged cyclophane **5** for single-crystal X-ray diffraction were obtained by slow evaporation of $CHCl_3$ at room temperature and their crystal structures are shown in Fig. 1.

The molecular structure of **5** clearly shows that this molecule has a basket-shaped structure with a 12 C alkyl tether connecting both N atoms of the QA core. Molecular **5** has a rather planar conformation, resembling the crystal structure of the non-bridged QA compounds reported in our previous work.[10] The geminal angles of the methylene in **5** are in the range of 112.5–116.9°, these angles are similar to each other and close to normal angles (Fig. S1, ESI†). The centroid distances between the QA ring and protons of the methylene tether are in the range of 3.40–4.0 Å which are larger than the van der Waals contact of H and C_{sp2} (2.9–3.1 Å), demonstrating that there is no obvious intramolecular C–H···π interaction in the 12 C tether bridged cyclophanes.

In the packing structures, the QA cyclophanes are readily π-overlapped with neighboring molecules, forming QA dimers

Table 1 Chemical shifts of selected protons of compounds **1–7** (500 MHz, $CDCl_3$, 1×10^{-4} M, rt)

Proton	**1**	**2**	**3**	**4**	**5**	**6**	**7**[a]
H_5 (ppm)	8.93	8.77	8.90	8.99	8.83	9.05	8.75
H_a (ppm)	0.15	0.28	0.13	0.29	0.37	0.26	1.12

[a] The highest chemical shift of the methylene proton.

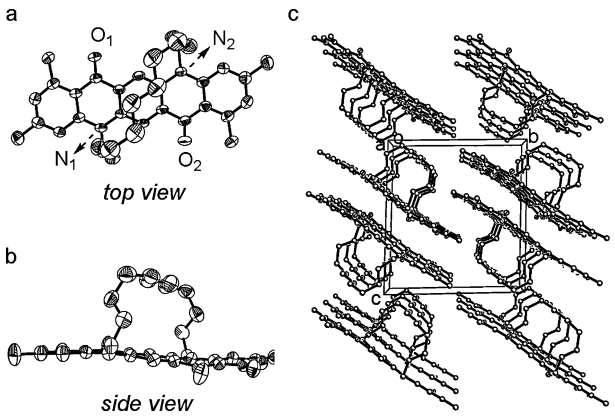

Fig. 1 Crystal structures of compound **5**: ORTEP drawings with 50% thermal ellipsoids: (a) top view and (b) side view; (c) packing structure of **5**.

with interfacial distance of about 3.5 Å. The dimers can not further aggregate due to the isolation effect of the bulky alkyl tethers, which is obviously different to the infinite π-stacking-featured molecular arrangements in normal QA derivatives. This molecular arrangement mode of QA cyclophanes might be of interest in terms of maintaining relatively high fluorescent quantum yields in the condensed phases.

Photophysical properties

The absorption and fluorescent spectra of QA cyclophanes **1–6** are measured in $CHCl_3$ (1×10^{-3} M), and their data are summarized in Table 2, together with those of QA reference **7** for comparison. As shown in Fig. 2a, the absorption spectra of all compounds showed two sets of absorption bands. Cyclophane **4** displays identical absorption profile to the reference **7** (λ_{max} for **7**: 491, 525 nm; **4**: 492, 525 nm). The absorption maxima of cyclophane **1** are red shifted by about 3 nm compared to that of **4**. In the same boat, cyclophanes **2** and **3** with distorted QA backbone show their absorption bands ranging from 489 to 535 nm, these bands are shifted to longer wavelength region by about 3 nm when compared to those of **5** and **6**. On the basis of the comparison of absorption maxima between 10 C tether bridged cyclophens **1–3** and 12C tether bridged ones **4–6**, a small redshift of 3 nm for all 10C tether bridged cyclophanes can be observed, this might be due to the polarity variation induced by the distortion of QA backbone or intramolecular C–H···π interactions in cyclophanes **1–3**. The two absorption bands of compound **1** are slightly red-shifted by about 8 nm compared to that of **2** (489 and 520 nm), and blue-shifted by about 8 nm compared to that of **3** (502 and 536 nm), demonstrating the substituted

Table 2 Photophysical data of QA cyclophanes **1–6** and QA derivative **7**[a]

	1	**2**	**3**	**4**	**5**	**6**	**7**
λ_{abs}/nm[b]	528	520	536	525	517	534	525
λ_{em}/nm[c]	557	555	569	554	550	566	573

[a] Measured in $CHCl_3$, $1–10^{-3}$ M. [b] Only longest absorption maxima are given. [c] Excited at 490 nm.

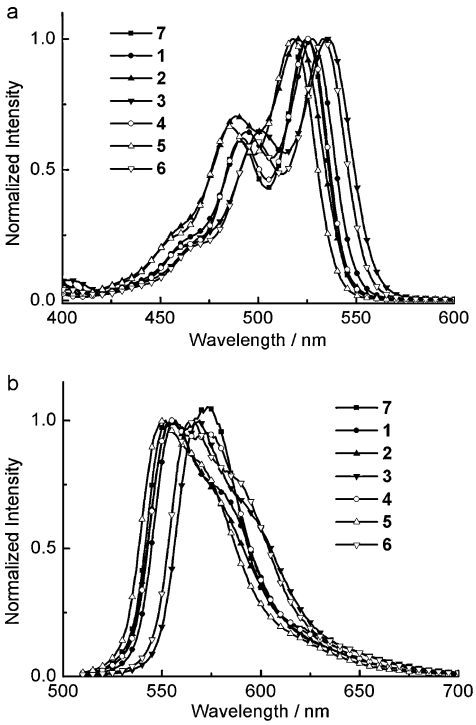

Fig. 2 UV-vis absorption (a) and fluorescent spectra (b) of QA cyclophanes **1–6** and QA derivative **7**.

effects on QA core. Similar trend can be observed in the comparison of absorption maxima among cyclophanes **4–6**.

Fig. 2b shows the fluorescent spectra of cyclophanes **1–6** and the reference compound **7**. All cyclophanes exhibit similar emission profiles with a shoulder in the longer wavelength region. The major difference between cyclophanes and the reference is that the stronger emission band of **7** appears at longer wavelength region due to strong π–π aggregation. The PL spectrum of **1** is slightly red-shifted compared with that of **4**, and similar observations were observed in the comparison between **2** and **5** and **3** and **6**. The conformational difference of QA backbone might be responsible for this difference. Substituted effects were also observed in the PL spectra of cyclophanes **1–6** and consistent with their absorption trend, for instance, the emission maxima of **4** is red-shifted by 4 nm compared with **5** and blue-shifted by 12 nm from **6**.

The X-ray crystal data indicate that the basket-shaped QA cyclophanes **1–6** have the ability to inhibit the formation of infinite face-to-face aggregates due to the isolation effect of the bridge, thus maintain the relatively high fluorescent quantum yields in condensed phase. To demonstrate this point, the concentration-dependent fluorescent quantum yields of **1–6** were measured, together with that of reference **7** for comparison. As shown in Fig. 3, all the compounds **1–7** are highly emissive in dilute solution (1×10^{-5} to 1×10^{-4} M) with Φ_F values over 0.80, demonstrating that substituents on QA backbone do not affect their fluorescent quantum yields in dilute solutions. The quantum yield of **7** dramatically decreases to 0.44 when the concentration increase to 2×10^{-4} M, indicative of a severe molecular aggregation. In contrast, the QA cyclophanes **1–6** still maintain the relatively high quantum yields (Φ_F: 0.70–0.86) at this concentration.

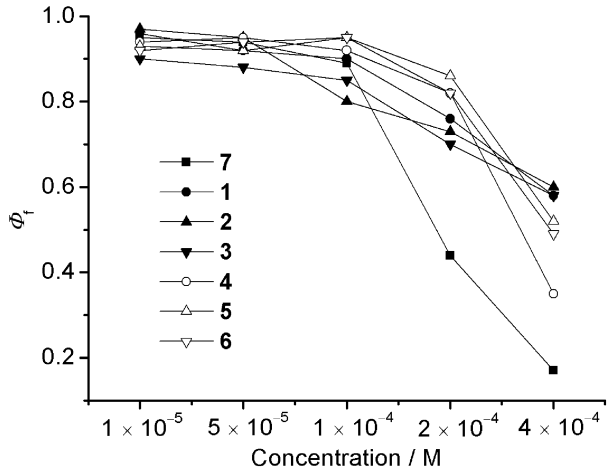

Fig. 3 Concentration-dependent fluorescent quantum yields of QA cyclophanes **1–6** and QA derivative **7**.

When further increasing the concentration to 4×10^{-4} M, the quantum yield of compound **7** decreases to 0.17, while most of cyclophanes have their quantum yields over 0.50. This result clearly demonstrates that the basket-shaped cyclophanes are indeed effective in inhibiting the intrinsic face-to-face π-aggregation of QA core which was thought to be the major reason for fluorescent quenching of QA dyes in the condensed phase. Concentration-dependent absorption behavior also supports this viewpoint. As shown in Fig. 4, cyclophane **1** do not display obvious aggregation upon increasing the concentration from 1×10^{-5} to 1×10^{-3} M. This is quite different to the concentration-dependent absorption behavior of reference compound **7** observed in our previous experiments.[10]

In addition, a comparison of the concentration-dependent fluorescent quantum yields among cyclophanes **1–6** gives more interesting information. As shown in Fig. 3, the quantum yields of 12C tether bridged cyclophanes **4–6** are in general lower than those of 10C tether bridged analogues **1–3** at high concentration (4×10^{-4} M) conditions. Compound **1–3** with 10C tether probably has a twisted QA core and forms crossed π-stacking dimers, and such a packing mode is effective to maintain a high quantum yield in crystalline state.[15] The conformation adopted by **1–3** in the solid state may be existed in solution and responsible for the higher quantum yields in the concentrated solution. It is noteworthy that the functionalization on the QA core is also important to keep high quantum yield in the condensed phases. As depicted in Fig. 3, the tetramethyl or di-butyl substituted cyclophanes **5** and **6** have relatively higher quantum yields compared to non-substituted cyclophane **4** at more concentrated conditions.

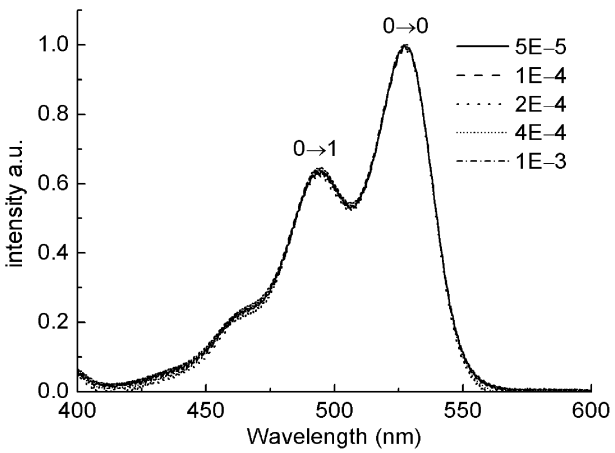

Fig. 4 Concentration-dependent absorption spectra of QA cyclophane **1**.

Electroluminescence

In our previous experiment, the luminescent efficiency of QA derivative **7** was very sensitive to the doping concentration. For instance, the luminance efficiency decreased by about 75% when increase the doping concentration from 0.5 to 3 wt%. To evaluate the potential application of these QA cyclophanes and investigate the effect of basket-shaped molecular structure on their electroluminescent property, we thus attempted to test the doping-concentration dependent electroluminescent behavior and chose cyclophane **1** for our device fabrication. The OLED device was fabricated by multilayer vapor deposition with the configuration of [ITO/NPB (600 Å)/Alq_3: **1** (500 Å)/LiF (10 Å)/Al (2000 Å)] where ITO (indium tin oxide) was the anode, *N*,*N*′-di(α-naphthyl)-*N*,*N*′-diphenyl-(1,1′-biphenyl)-4,4′-diamine (NPB) served as a hole transport layer, ti-(8-hydroxyquinolino)aluminium (Alq_3) doped with **1** as emitting layer, Alq_3 as an electron transport layer, and LiF/Al as the composite cathode. For the comparison

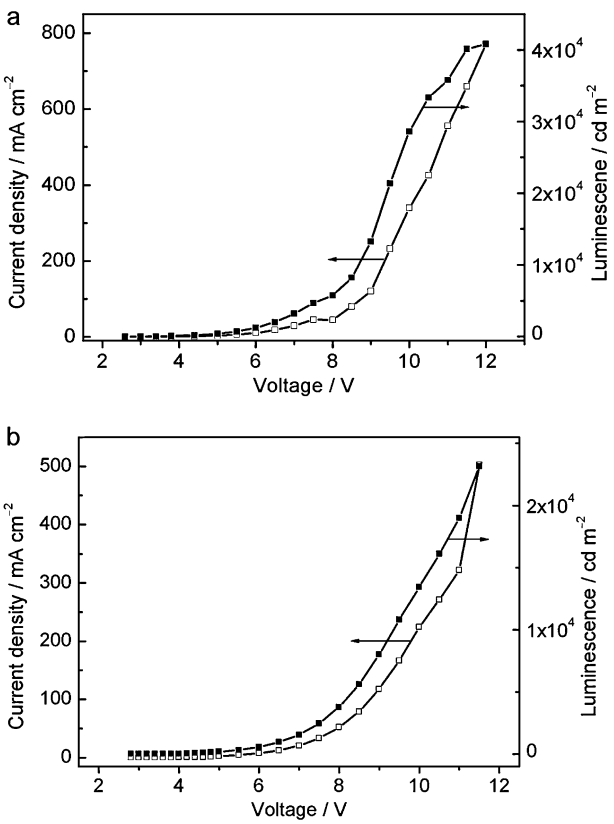

Fig. 5 The current–voltage–luminance curves of (a) device A and (b) device B.

purposes we fabricated two devices A and B with doping concentrations of 0.5 wt% for the former and 3 wt% for latter.

We obtained green emissions from both devices A and B that were identical to the PL spectrum of **1** in solution and noted that the EL originated only from QA compound (Fig. S2, ESI†). The current density–voltage and luminance–voltage characteristics of devices A and B are displayed in Fig. 5. The maximum luminance efficiencies of devices A and B are 11.2 cd A^{-1} (brightness: 352 cd m^{-2}; driving voltage: 6.5 V) and 7.2 cd A^{-1} (brightness: 296 cd m^{-2}; driving voltage: 6.5 V), respectively. On the basis of this data, only 35% of efficiency decrease was observed upon increasing doping concentration from 0.5 to 3 wt%, further demonstrating that the basket-shaped functionalization of QA dyes is effective to inhibit molecular aggregation in the condensed phase.

Conclusion

In summary, a series of basket-shaped QA cyclophanes **1–6** was prepared and characterized. X-Ray crystal analysis of compound **5** indicates that this type of structure facilitates QA dyes to form π-stacked dimers. In the condensed phases, the sterically bulky bridging tether on both sides of the produced dimers effectively inhibits the formation of infinite face-to-face π-stacking aggregation that is an arrangement feature observed in normal QA derivatives. All QA cyclophanes exhibited much higher fluorescent quantum yields compared to the reference QA compound **7** at the concentrated conditions, reflecting that our design strategy was indeed effective to decrease the fluorescent quenching of QA dyes. Doping-concentration-dependent luminance efficiencies of EL devices based on cyclophane **1** further support that the basket-shaped structure has the ability to effectively keep QA core apart. We believe that the present molecular design strategy is not only suitable for achieving highly luminescent QA dyes but also suitable for other planar luminescent organic dyes which are usually suffer from the fluorescent quenching problem in the condensed phase.

Experimental

Materials

Quinacridone (QA) was purchased from Tokyo Kasei Kogyo Co. 1,3,8,10-tetramethyl-quinacridone (TMQA) and 2,9-ditertubitylquinacridone (DBQA) were synthesized according to literature.[9c,10] 1,10-Dibromodecane and 1,12-dibromododecane were purchased from Acros. Alq_3 was purchased from Aldrich and purified by vacuum sublimation. NPB was synthesized according to the literature procedures.[16] Solvents were freshly distilled over appropriate drying reagents. THF was distilled from sodium/benzophenone ketyl under nitrogen atmosphere immediately prior to use. All experiments were carried out under a dry nitrogen atmosphere using standard Schlenk techniques unless otherwise stated. The synthetic procedures of QA cyclophanes are shown in Scheme 2.

Instrumentation

^{1}H NMR spectra were recorded on Bruker AVANCE 500 MHz spectrometer with tetramethylsilane as the internal standard. Mass spectra were recorded on a GC-MS mass spectrometer. Absorption spectra were obtained using a PE UV-VIS Lambda 20 spectrometer. Elemental analyses were performed on a Flash EA 1112 spectrometer. Photoluminescence spectra were collected by a Shimadzu RF-5301PC spectrophotometer. The melting points were determined on a Fisher-Johns melting point apparatus.

Photoluminescence measurements

The room temperature luminescence quantum yields were measured at a single excitation wavelength (360 nm) referenced to quinine sulfate in sulfuric acid aqueous solution (Φ_F = 0.546). The quantum yields were calculated using previously known procedures.[4] The excitation wavelength was 490 nm for all QA cyclophanes **1–6** and reference **7**.

Fabrication of EL devices

Indium-tin oxide (ITO) coated glass was used as the substrate. It was cleaned by sonication successively in a detergent solution, acetone, methanol, and deionized water before use. The devices were prepared in vacuum at a pressure of 5×10^{-6} torr. Organic layers were deposited onto the substrate at a rate of 1–2 Å s^{-1}. After the organic film deposition, LiF and aluminium were thermally evaporated onto the organic surface. The thicknesses of the organic materials and the cathode layers were controlled using a quartz crystal thickness monitor. The electrical characteristics of the devices were measured with a Keithley 2400 source meter. The EL spectra and luminance of the devices were obtained on a PR650 spectrometer.

X-ray crystallography

Diffraction data were collected on a Rigaku R-AXIS RAPID diffractometer (Mo-Kα radiation, graphite monochromator) in the Ψ rotation scan mode. The structure determination was done with direct methods by using SHELXL 5.01v and refinements with full-matrix least squares on F^2. The positions of hydrogen atoms were calculated and refined isotropically. Crystal data for **5**: CCDC 759654; $C_{36}H_{42}N_2O_2$; FW = 534.72, Triclinic, $P\bar{1}$, a = 8.3832(2) Å, b = 12.547(3) Å, c = 13.805(3) Å, α = 87.60(3)°, β = 83.31(3)°, γ = 85.67(3)°, V = 1437.3(5) $Å^3$, Z = 2, D_c = 1.236 g cm^{-3}. The refinement converged to R_1 = 0.0726, wR_2 = 0.2037 ($I > 2\sigma(I)$), GOF = 0.927.

Synthesis

Cyclophane 1. Under nitrogen, sodium hydride (1.0 g, 42 mmol) was added to a suspension of quinacridone (0.31 g, 1 mmol) in 500 mL of dry tetrahydrofuran (THF). The mixture was heated to reflux for 1 h then 1,10-dibromodecane (0.30 g, 1 mmol) was added. The reaction mixture was continued to heat to reflux overnight. After distilling off excess of 1,10-dibromodecane and THF, methanol (50 mL) was added dropwise to the reaction mixture. The resulting suspension was stirred for 1 h. The generated orange precipitate was filtered and washed with methanol. After drying, the crude cyclophane **1** was obtained in 22% yield, which was purified by column chromatography using silica gel

with chloroform as eluent to yield 95 mg (21%). ^{1}H NMR (500 MHz, $CDCl_3$, 25 °C, TMS): δ = 8.93, (s, 2H), 8.61 (d, J = 8.0 Hz, 2H), 7.77 (t, J = 7.0 Hz, 2H), 7.63 (d, J = 8.5 Hz, 2H), 7.30 (t, J = 7.5 Hz, 2H), 5.01–4.95 (m, 2H), 4.72–4.67 (m, 2H), 1.98–1.92 (m, 2H), 1.82–1.75 (m, 2H), 1.05–0.98 (m, 2H), 0.64–0.55 (m, 4H), 0.43–0.40 (m, 2H), 0.31–0.24 (m, 2H), 0.17–0.12 (m, 2H); Mp > 300 °C; Ms: m/z: 450.0 $[M]^+$; element analysis calcd (%) for $C_{30}H_{30}N_2O_2$: C 79.97, H 6.71, N 6.22; found: C 80.0, H 6.69, N 6.23.

Cyclophane 2. In the same manner as described for **1**, 1, 3, 8, 10-tetramethylquinacridone (TMQA) (0.37 g, 1.0 mmol) react with 1,10-dibromodecane (0.30 g, 1.0 mmol) according to the procedure described for the synthesis of **1** to yield 86 mg (17%) **2**. ^{1}H NMR (500 MHz, $CDCl_3$, 25 °C, TMS): δ = 8.77, (s, 2H), 7.24 (s, 2H), 6.87 (s, 2H), 4.93–4.87 (m, 2H), 4.62–4.57 (m, 2H), 2.98 (s, 6H), 2.48 (s, 6H), 1.92–1.85 (m, 2H), 1.84–1.76 (m, 2H), 1.07–0.99 (m, 2H), 0.63–0.55 (m, 4H), 0.48–0.37 (m, 4H), 0.30–0.25 (m, 2H); Mp: 261–263 °C; Ms: m/z: 506.0 $[M]^+$; element analysis calcd (%) for $C_{34}H_{38}N_2O_2$: C 80.63, H 7.51, N 5.53; found: C 80.57, H 7.74, N 5.33.

Cyclophane 3. In the same manner as described for **1**, 2,9-ditertubitylquinacridone (DBQA) (0.42 g, 1.0 mmol) react with 1,10-dibromodecane (0.30 g, 1.0 mmol) according to the procedure described for the synthesis of **1** to yield 84 mg (15%) **3**. ^{1}H NMR (500 MHz, $CDCl_3$, 25 °C, TMS): δ = 8.90, (s, 2H), 8.57 (s, 2H), 7.82 (d, J = 9.0 Hz, 2H), 7.56 (d, J = 9.5 Hz, 2H), 4.93–4.99 (m, 2H), 4.64–4.70 (m, 2H), 2.00–1.92 (m, 2H), 1.80–1.73 (m, 2H), 1.44 (s, 18H), 1.04–0.96 (m, 2H), 0.64–0.54 (m, 4H), 0.46–0.39 (m, 2H), 0.28–0.22 (m, 2H), 0.18–0.09 (m, 2H); Mp > 300 °C; Ms: m/z: 562.0 $[M]^+$; element analysis calcd (%) for $C_{38}H_{46}N_2O_2$: C 81.14, H 8.19, N 4.98; found: C 81.0, H 8.25, N 4.92.

Cyclophane 4. In the same manner as described for **1**, quinacridone (0.31 g, 1.0 mmol) react with 1,12-dibromododecane (0.36 g, 1.0 mmol) according to the procedure described for the synthesis of **2** to yield 105 mg (22%) **4**. ^{1}H NMR (500 MHz, $CDCl_3$, 25 °C, TMS): δ = 8.99, (s, 2H), 8.62 (d, J = 8.0 Hz, 2H), 7.76 (t, J = 8.0 Hz, 2H), 7.64 (d, J = 8.5 Hz, 2H), 7.31 (t, J = 7.5 Hz, 2H), 5.05–5.00 (m, 2H), 4.69–4.64 (m, 2H), 2.03–1.99 (m, 4H), 1.14–1.07 (m, 2H), 0.92–0.86 (m, 4H), 0.78–0.66 (m, 6H), 0.53–0.45 (m, 2H), 0.32–0.26 (m, 2H); Mp > 300 °C; Ms: m/z: 478.0 $[M]^+$; element analysis calcd (%) for $C_{32}H_{34}N_2O_2$: C 80.33, H 7.11, N 5.86; found: C 80.08, H 7.37, N 5.68.

Cyclophane 5. In the same manner as described for **1**, 1, 3, 8, 10-tetramethylquinacridone (TMQA) (0.37 g, 1.0 mmol) react with 1,12-dibromododecane (0.36 g, 1.0 mmol) according to the procedure described for the synthesis of **1** to yield 101 mg (19%) **5**. ^{1}H NMR (500 MHz, $CDCl_3$, 25 °C, TMS): δ = 8.83 (s, 2H), 7.25 (s, 2H), 6.87 (s, 2H), 5.00–4.95 (m, 2H), 4.58–4.54 (m, 2H), 2.99 (s, 6H), 2.48 (s, 6H), 2.08–2.00 (m, 2H), 1.93–1.86 (m, 2H), 1.12–1.05 (m, 2H), 0.95–0.85 (m, 4H), 0.81–0.74 (m, 6H), 0.57–0.51 (m, 2H), 0.40–0.34 (m, 2H); Mp > 300 °C; Ms: m/z: 534.0 $[M]^+$; element analysis calcd (%) for $C_{36}H_{42}N_2O_2$: C 80.90, H 7.88, N 5.24; found: C 80.60, H 8.00, N 5.08. X-ray-quality crystals were grown by slow diffusion of diethyl ether vapor into a chloroform solution of **1**.

Cyclophane 6. In the same manner as described for **1**, 2,9-ditertubitylquinacridone (DBQA) (0.42 g, 1.0 mmol) react with 1,12-dibromodecane (0.36 g, 1.0 mmol) according to the procedure described for the synthesis of **1** to yield 100 mg (17%) **6**. ^{1}H NMR (500 MHz, $CDCl_3$, 25 °C, TMS): δ = 9.05, (s, 2H), 8.61 (s, 2H), 7.85 (d, J = 8.5 Hz, 2H), 7.62 (d, J = 9.0 Hz, 2H), 5.09–5.03 (m, 2H), 4.69–4.66 (m, 2H), 2.04–2.00 (m, 2H), 1.45 (s, 18H), 1.14–1.07 (m, 2H), 0.93–0.86 (m, 4H), 0.80–0.65 (m, 6H), 0.51–0.44 (m, 2H), 0.29–0.22 (m, 2H); Mp > 300 °C; Ms: m/z: 590.0 $[M]^+$; element analysis calcd (%) for $C_{40}H_{50}N_2O_2$: C 81.35, H 8.48, N 4.74; found: C 81.64, H 8.69, N 4.49.

Acknowledgements

This work was supported by the National Natural Science Foundation of China (50733002, 50903037, and 50773027), the Major State Basic Research Development Program (2009CB623600) and 111 Project (B06009).

References

1 (*a*) M. Hiramoto, S. Kawase and M. Yokoyama, *Jpn. J. Appl. Phys.*, 1996, **35**, L349; (*b*) T. Shichiri, M. Suezaki and T. Inoue, *Chem. Lett.*, 1992, 1717; (*c*) H. Nakahara, K. Kitahara, H. Nishi and K. Fukuda, *Chem. Lett.*, 1992, 711; (*d*) H. Nakahara, K. Fukuda, M. Ikeda, K. Kitahara and H. Nishi, *Thin Solid Films*, 1992, **210–211**, 555; (*e*) P. Liu, C.-P. Chang and H. Tian, *Proc. SPIE*, 2002, **4464**, 299; (*f*) P.-H. Liu, H. Tian and C.-P. Chang, *J. Photochem. Photobiol., A*, 2000, **137**, 99; (*g*) E. M. Gross, J. D. Anderson, A. F. Slaterbeck, S. Thayumanavan, S. Barlow, Y. Zhang, S. R. Marder, H. K. Hall, M. F. Nabor, J. F. Wang, E. A. Mask, N. R. Armstrong and R. M. Wightman, *J. Am. Chem. Soc.*, 2000, **122**, 4972.
2 (*a*) U. Keller, K. Müllen, S. De Feyter and F. C. De Schryver, *Adv. Mater.*, 1996, **8**, 490; (*b*) S. De Feyter, A. Gesquiére, F. C. De Schryver, U. Keller and K. Müllen, *Chem. Mater.*, 2002, **14**, 989.
3 S. E. Shaheen, B. Kippelen, N. Peyghambarian, J. F. Wang, J. D. Anderson, E. A. Mash, P. A. Lee, N. R. Armstrong and Y. J. Kawabe, *J. Appl. Phys.*, 1999, **85**, 7939.
4 W. H. Flora, H. K. Hall and N. R. Armatrong, *J. Phys. Chem. B*, 2003, **107**, 1142.
5 A. W. Freeman, S. C. Koene, P. R. L. Malenfant, M. E. Thompson and J. M. J. Frechet, *J. Am. Chem. Soc.*, 2000, **122**, 12385.
6 J. Shi and C. W. Tang, *Appl. Phys. Lett.*, 1997, **70**, 1665.
7 T. Wakimoto, Y. Yonemoto, J. Funaki, M. Tsuchida, R. Murayama, H. Nakada, H. Matsumoto, S. Yamamura and M. Nomura, *Synth. Met.*, 1997, **91**, 15.
8 H. Aziz, Z. D. Popovic and N. Hu, *Appl. Phys. Lett.*, 2002, **81**, 370.
9 (*a*) D. Qiu, K. Ye, Y. Wang, B. Zhou, X. Zhang, S. B. Lei and L. J. Wan, *Langmuir*, 2003, **19**, 678; (*b*) Z. Mu, Z. Wang, X. Zhang, K. Ye and Y. Wang, *Langmuir*, 2004, **20**, 8892; (*c*) F. D. Lin, Y. Zhong, L. F. Chi, K. Ye, Y. Wang and H. Fuchs, *Phys. Rev. B*, 2006, **73**, 235420; (*d*) J. Wang, Y. Zhao, C. Dou, H. Sun, P. Xu, K. Ye, J. Zhang, S. Jiang and Y. Wang, *J. Phys. Chem. B*, 2007, **111**, 5082; (*e*) J. Wang, Y. Zhao, J. Zhang, J. Zhang, B. Yang, Y. Wang, D. Zhang, H. You and D. Ma, *J. Phys. Chem. C*, 2007, **111**, 9177; (*f*) Y. Zhao, Y. Fan, X. Mu, H. Gao, J. Wang, J. Zhang, W. Yang, L. Chi and Y. Wang, *Nano Res.*, 2009, **2**, 493.
10 K. Ye, J. Wang, H. Sun, Y. Liu, Z. Mu, F. Li, S. Jiang, J. Zhang, H. Zhang, Y. Wang and C. Che, *J. Phys. Chem. B*, 2005, **109**, 8008.
11 J. B. Briks, in *Photophysics of Aromatic Molecules*, Wiley, London, 1970.
12 (*a*) Y. Ooyama, T. Nakamura and K. Yoshida, *New J. Chem.*, 2005, **29**, 447; (*b*) G. R. Desiraju, *Angew. Chem., Int. Ed.*, 2007, **46**, 8342; (*c*) L. R. MacGillivray, *Nature*, 2008, **451**, 897; (*d*) R. Davis,

N. S. S. Kumar, S. Abraham, C. H. Suresh, N. P. Rath, N. Tamaoki and S. Das, *J. Phys. Chem. C*, 2008, **112**, 2137; (*e*) N. S. S. Kumar, S. Varghese, N. P. Rath and S. Das, *J. Phys. Chem. C*, 2008, **112**, 8429; (*f*) C. Bazzini, T. Caronna, F. Fontana, P. Macchi, A. Mele, I. N. Sora, W. Panzeri and A. Sironi, *New J. Chem.*, 2008, **32**, 1710; (*g*) J. Dong, K. M. Solntsev and L. M. Tolbert, *J. Am. Chem. Soc.*, 2009, **131**, 662; (*h*) K. Shiraishi, T. Kashiwabara, T. Sanji and M. Tanaka, *New J. Chem.*, 2009, **33**, 1680.

13 (*a*) H. Zhang, Z. Zhang, K. Ye, J. Zhang and Y. Wang, *Adv. Mater.*, 2006, **18**, 2369; (*b*) Y. Zhao, H. Gao, Y. Fan, T. Zhou, Z. Su, Y. Liu and Y. Wang, *Adv. Mater.*, 2009, **21**, 3165.

14 (*a*) G. J. Bodwell, J. J. Fleming, M. R. Mannion and D. O. Miller, *J. Org. Chem.*, 2000, **65**, 5360; (*b*) G. J. Bodwell, J. N. Bridson, M. K. Cyrański, J. W. J. Kennedy, T. M. Krygowski, M. R. Mannion and D. O. Miller, *J. Org. Chem.*, 2003, **68**, 2089; (*c*) G. J. Bodwell, J. N. Bridson, S.-L. Chen and R. A. Poirier, *J. Am. Chem. Soc.*, 2001, **123**, 4704.

15 Z. Xie, B. Yang, F. Li, G. Cheng, L. Liu, G. Yang, H. Xu, L. Ye, M. Hannif, S. Liu, D. Ma and Y. Ma, *J. Am. Chem. Soc.*, 2005, **127**, 14152.

16 B. E. Koene, D. E. Loy and M. E. Thompson, *Chem. Mater.*, 1998, **10**, 2235.